PRAMANA
— journal of
physics

Vol. 67, No. 1
July 2006
pp. 199–205

Ballistic transport in semiconductor nanostructures: From quasi-classical oscillations to novel THz-emitters

G H DÖHLER[1,2], M ECKARDT[2], A SCHWANHÄUßER[2], F RENNER[2], S MALZER[1,2], S TRUMM[3], M BETZ[3], F SOTIER[3,4], A LEITENSTORFER[3,4], G LOATA[5], T LÖFFLER[5], H ROSKOS[5], T MÜLLER[6], K UNTERRAINER[6], D DRISCOLL[7], M HANSON[7] and A C GOSSARD[7]

[1]Max-Planck-Research Group of Optics, Information and Photonics, Günther-Scharowski-Strasse 1, Bau 24, University of Erlangen, 91058 Erlangen, Germany
[2]Institute of Technical Physics I, Erwin-Rommel-Strasse 1, University of Erlangen, 91058 Erlangen, Germany
[3]Physik-Department E 11, Technische Universität München, 85748 Garching, Germany
[4]Fachbereich Physik, Universität Konstanz, 78457 Konstanz, Germany
[5]Institute of Physics, Johann Wolfgang Goethe University, Max-von-Laue-Str. 1, 60438 Frankfurt, Germany
[6]Institut für Festkörperelektronik, Technische Universität Wien, Vienna, Austria
[7]Materials Department, University of California, Santa Barbara, CA 93106, USA
E-mail: dohler@physik.uni-erlangen.de

Abstract. By suitable design it is possible to achieve quasi-ballistic transport in semiconductor nanostructures over times up to the ps-range. Monte-Carlo simulations reveal that under these conditions phase-coherent real-space oscillations of an electron ensemble, generated by fs-pulses become possible in wide potential wells. Using a two-color pump-and-probe technique we have been able to observe this new phenomenon in excellent agreement with the theoretical predictions. Apart from its fundamental significance, ballistic transport in nanostructures can also be used for high-efficiency coherent THz-sources. The concept of these THz-emitters and its experimental confirmation will also be presented.

Keywords. Ultrashort laser pulses; semiconductor nanostructures; ballistic transport.

PACS Nos 42.65.Re; 73.23.Ad; 73.50.Fq; 73.50.Gr; 42.65.Re

1. Introduction

Femtosecond (fs) laser pulses represent an ideal tool for the investigation of the dynamics of non-thermal carriers in solids. By probing reflectance or transmission changes of a 'probe pulse' at a certain delay time t after excitation by a 'pump pulse', one can monitor the changes of optical properties induced by the light-induced carriers. As the delay time can be varied easily through a variation of the path

length of the probe beam, the time resolution does not depend on the response time of the detector. The time resolution is only determined by the pulse width and the jitter between pump and probe pulse. This jitter can be extremely small if both beams stem from the same laser. Even in this case it is possible to obtain pulses with different width and center frequencies [1], which allows for '2-color pump-and-probe' experiments. As the pulse energies are reasonably high and repetition rates are typically in the range of 80 MHz, the measurements exhibit very low noise. Therefore, very small transmission or reflection changes can be easily resolved. This technique has been widely used for studies of the dynamics of hot carriers in solids on a fs-scale [2]. Although the same method can also be used for the study of non-stationary transport phenomena, its potential has hardly been exploited [3]. Recently, we have performed 2-color pump-and-probe fs-experiments on semiconductor nanostructures with the aim of studying the non-stationary transport of photo-generated carriers in high electric fields. Our sample design allows us to obtain both temporally and spatially resolved information about the evolution of the density distribution $n(z,t)$ in an ensemble of electrons (or holes) under the influence of an electric field F in the z-direction. In all our studies to be summarized below, we have been using GaAlAs p–i–n or similar diodes. In order to confine the generation of electrons and holes to a narrow spatial region we have used the 'trick' of graded band gaps, which can be easily implemented by ramping up the Al-content from zero to relatively small values. This way absorption and, thus, carrier generation takes place only within about 10 nm around the region with the smallest band gap. In our first series of experiments (see §2) we have studied the 'transient transport' due to electrons (or holes) generated close to the band edge in (quasi)-uniform semiconductor bulk material. This allowed us, in particular, to investigate in detail the ballistic flight of electrons in the Γ-valley with low effective mass at short times, followed by deceleration after intervalley transfer to the L- and X-valleys. Our second effort (see §3) was to suppress intervalley scattering by a suitable sample design. In these structures the carriers are confined within (rather wide) potential wells, in which the electrons can never gain the minimum energy required for intervalley scattering. Therefore, the transport remains quasi-ballistic over several ps and the electrons perform quasi-classical oscillations in the THz-range over several periods. This is a new phenomenon, different from 'quantum beats', which we have demonstrated for the first time. Finally, in §4 we have used ballistic transport for the generation of continuous wave (c.w.) THz-radiation. In these 'photomixers' the pulsed laser is replaced by two lasers of the same intensity, but de-tuned by the THz-frequency and the diode structures are replaced by cascaded nano-nip-diodes ('nipnip-photomixer'). As all this work has been published recently we confine ourselves here to a short outline of each of these projects.

2. Ultrafast transport in GaAs

The design and a real-space band diagram of the pin-diode are shown schematically in figure 1. In the upper part the spatial variation of the Al-content is depicted. The p- and n-contact layers ($z < 0$ and $z > 900$ nm, respectively) are non-absorbing as the band gap exceeds both the pump and probe laser photon energy. Absorption takes place very near to $z = 0$. As the holes are already at the p-contact

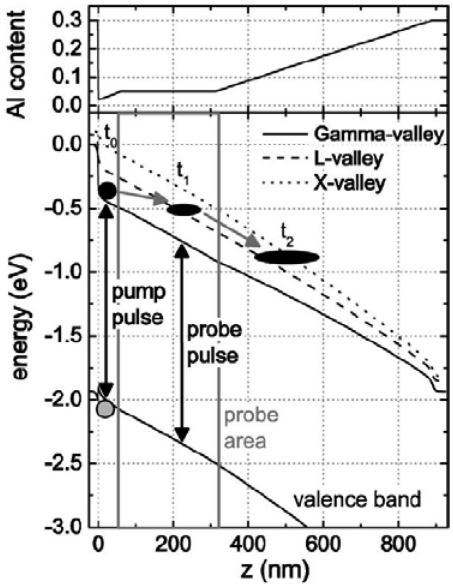

Figure 1. Schematic band structure of the p–i–n heterostructure under zero applied bias U. A bias applied between the (left) p- and (right) n-contacts results in a change of the (stationary) electric field in the intrinsic region. The interband transitions used for generation of the electron ensemble (near $z = 0$) and its detection (within the range 60 nm $< z <$ 320 nm) are indicated by arrows. The delay times t_0, t_1 and t_2 represent different stages in the evolution of the electron distribution. The upper part of the figure depicts the aluminum content within the heterostructure.

they do not contribute to the transport at all. Therefore, this design allows us to study electron transport alone. By the application of an external voltage between p- and n-contact the field experienced by the electrons can be modified. At low fields (significantly lower than shown in the figure) the electron ensemble generated by the pump pulse can travel ballistically (i.e. keeping its original position on the energy axis) with velocities up to 10^8 cm/s while propagating over a distance of 100 nm or so before reaching the (local) energy of the L-valley band edge and being slowed down to the 'saturation velocity' of about 10^7 cm/s. Whereas the acceleration at higher fields becomes even faster, the slow-down sets in earlier. Therefore, the electron ensemble may enter the region (marked 'probe area') (60 nm $< z <$ 320 nm) earlier at higher fields but the transit time for reaching its right boundary ($z = 320$ nm) is expected to increase (!) at higher fields. Information about the transit of the electrons through the probe area via the probe beam is due to the Franz–Keldysh effect (FKE). According to the FKE the absorption spectrum of a semiconductor near the band edge is field-dependent. When the electrons pass through the probe area, the dipole field between the electrons and the (same number of) holes generated at $z = 0$ partially screens the built-in field. This is reflected in the pump-and-probe experiments as a clear change of the transmission spectra, which reaches saturation when the last electrons leave the probe area. In order

to compare experiment and theory we have performed Monte-Carlo simulations of the transport and the resulting transmission changes as a function of delay time t. Perfect agreement is obtained, if the temporal and spatial broadening of the electron distribution is taken into account and if appropriate values for the relevant material parameters are used in the simulation. Regarding the material parameters most of them are well established. However, our simulations reveal that the agreement with experiment is quite sensitive to the choice of the intervalley deformation potential, for which a wide range of values has been reported in the literature. Thus, our study provides new information regarding the correct value for this important parameter ([4]; note that, unfortunately, the graphs for figures 7 and 8 are interchanged). The temporal and spatial broadening of the electron distribution mentioned above has an important consequence on the high-frequency behavior of ultrafast photodetectors.

Our sample design allows us to also study the hot-hole transport (free from any disturbing electron contributions) if an 'inverted' structure design is used (with n- and p-layer interchanged). This way we have been able to measure the field- and temperature dependence of hot electrons again providing additional important insight for the design of ultrafast photodetectors [5].

3. Semiclassical real-space oscillations

As mentioned in the introduction, the deceleration of ballistic electrons can be prevented, if the electrons do not gain sufficiently high kinetic energy from the potential for intervalley scattering to become possible. Such a scenario is shown in figure 2b. Electrons starting an ideal ballistic flight (no scattering, no energy dissipation) at the left corner ($z = 50$ nm) will gain a little less energy than necessary for scattering into the L-valley till they reach the center of the potential well ($z = 175$ nm). Therefore, they will continue their ballistic trajectory, but they are now smoothly decelerated until they reach the turning point on the right side. The dots shown in figure 2b indicate the center-of-mass position in energy and real space, taken at time intervals of 16 fs, for an electron ensemble generated at $t = 0$ at $z = 50$ nm as obtained from a realistic ensemble Monte-Carlo simulation, which takes into account all relevant scattering mechanisms. Although the ensemble looses energy at a significant rate due to the emission of optical phonons, the phase coherence of the oscillations in real-space gets lost only after several oscillation periods. This is due to the fact that the scattering process with longitudinal optical phonons (LO) favors small-angle scattering. This means that, although the energy decreases by $h\nu_{\mathrm{LO}}$ in each scattering event, the direction of the velocity vector remains nearly unchanged and the oscillation with a frequency $\omega = (C/m_c)^{1/2}$ persists (C being the curvature of the parabolic potential well and m_c the effective electron mass). A similar simulation performed for a significantly deeper potential well (figure 2c) results in a monotonous relaxation of the carriers towards the center of the potential well at $z = 175$ nm. The latter case corresponds to the familiar transport scenario, where the frictional term dominates over the inertial term in the classical Drude equation of motion. The case shown in figure 2b, however, represents a new regime of classical transport, where the inertial term dominates over the frictional one. Note that the resulting oscillations in real space (in contrast to the well-known

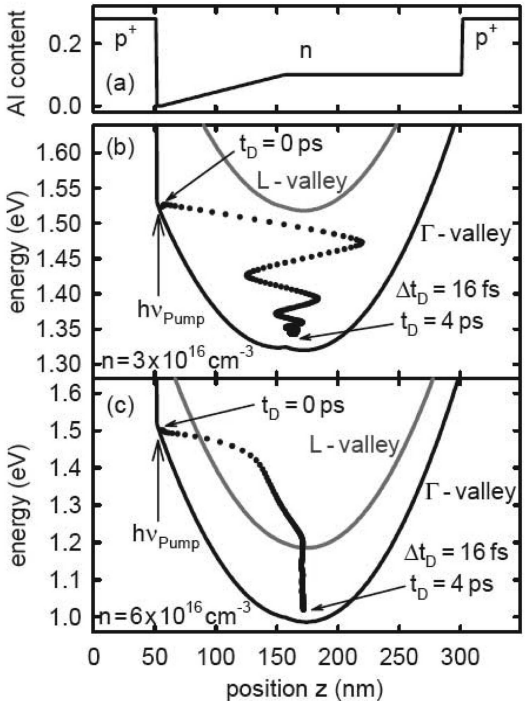

Figure 2. Band structure of the p–n–p heterostructures used for the demonstration of novel quasi-classical ballistic THz-oscillations. The dots represent the results of realistic Monte-Carlo simulations for the energy and real-space position of the center-of-mass of the electron ensemble generated at the left corner at $t = 0$, taken at time intervals of 16 fs. For details see text.

Bloch oscillations in k-space) represent a predominantly classical phenomenon. The spacing of energy eigenstates $h\nu$ in a quantum mechanical treatment of the system would correspond to a fraction of $h\nu_{\mathrm{LO}}$ only. That means that a single scattering event corresponds to a scattering into a state separated in energy by several quanta $h\nu$.

We have implemented this concept by fabricating a p–n–p AlGaAs-heterostructure with a graded Al-content and, hence, a graded band gap for 50 nm $< z <$ 175 nm. The parabolic potential is due to the positive space charge of the ionized donors. Our pump-and-probe experiments have fully confirmed the predictions obtained from the Monte-Carlo simulations and, thus demonstrated this novel phenomenon [6].

4. Ballistic-electron THz-emitter

The frequency of the oscillations discussed in the previous section is typically in the THz range. The phase-coherent oscillation of an ensemble of electrons corresponds

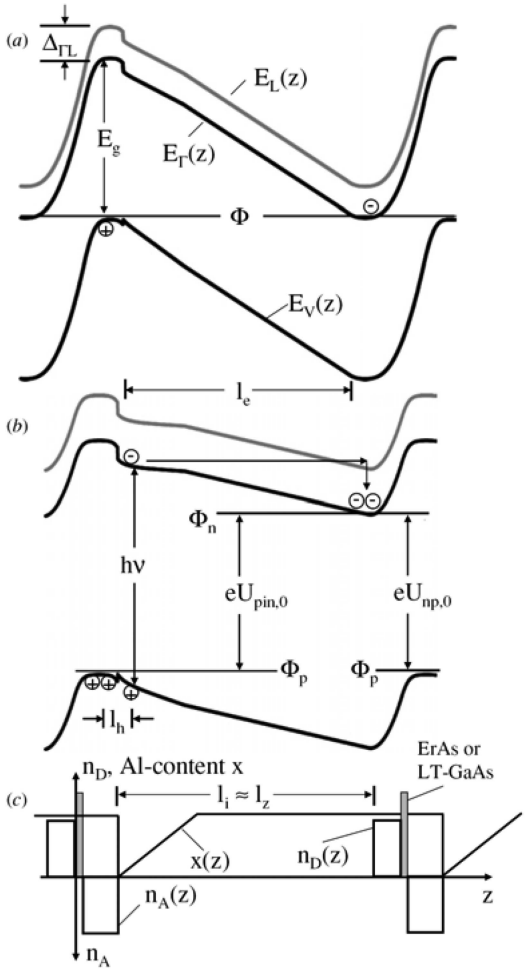

Figure 3. One period of the cascaded nanopin diodes used for our photomixer for the generation of c.w. THz-radiation. (**c**) Doping profiles and spatial variation of Al-content. (**a**) The resulting band diagram in the dark state and (**b**) under optimum operation conditions. The (periodically oscillating) electron photocurrent generated in the left corner of the pin diode is balanced, on the average, by the (basically constant) recombination within the ErAs layer of the n–p recombination diode with the holes generated in the neighboring pin diode to the right

to a macroscopic THz-current. This current can be detected via the electromagnetic radiation emitted by the coherent acceleration and deceleration of the electron ensemble [6] or by the radiation emitted via an antenna, if the THz-displacement current induced in the contacts is fed into the antenna, resulting in an attenuated oscillatory THz-radiation pulse in both cases. The generation of continuous wave (c.w.) THz-radiation is possible, in principle, by using two c.w. lasers emitting with

the same intensity at two photon frequencies differing from each other just by the THz-frequency. This results in a (fully modulated) periodic carrier generation. If this generation frequency is in resonance with the THz-oscillation frequency of the potential well maximum THz-emission is expected from a simple-minded consideration. Unfortunately, the accumulation of a quasi-steady-state electron density near the center of the potential well disturbs this resonant oscillation. The reason is a too slow recombination of the photogenerated electrons (being collected at the center of the well) with the spatially separated holes (collected at the p-contact layers). To overcome this problem, we have designed multi-period nipn-structures as depicted in figure 3. The p–n junctions contain a layer of ErAs, which forms nanosize clusters and serves as a very efficient recombination center. Although the advantage of periodic oscillations is abandoned in this scheme, this emitter design appears to be the most appealing one among the THz-photomixer proposed and realized so far. This assertion is elaborated in detail in ref. [7]. In this reference also experimental evidence from experiments on such photomixers with antenna is provided, demonstrating the advantage of the ballistic regime, which results in a much slower high-frequency roll-off compared to the other approaches pursued for photomixers (photoconductive mixer and even other sophisticated pin-mixer).

References

[1] C Fürst, A Leitenstorfer and A Laubereau, *IEEE J. Sel. Top. Quantum Electron.* **2**, 473 (1996)

[2] See, for instance, J Shah, *Ultrafast spectroscopy of semiconductors and semiconductor nanostructures* (Springer, Berlin, 1999)

[3] A Leitenstorfer, S Hunsche, J Shah, M C Nuss and W H Knox, *Phys. Rev. Lett.* **82**, 5140 (1999)

[4] A Schwanhäußer, M Betz, M Eckardt, S Trumm, L Robledo, S Malzer, A Leitenstorfer and G H Döhler, *Phys. Rev.* **B70**, 085211 (2004)

[5] S Trumm, M Betz, F Sotier, A Leitenstorfer, A Schwanhäuer, M Eckardt, S Malzer, M Hanson, D Driscoll, A C Gossard and G H Döhler, *Appl. Phys. Lett.* **86**, 142105 (2005)

[6] M Eckardt, M Betz, A Schwanhäußer, S Trumm, F Sotier, L Robledo, S Malzer, T Müller, K Unterrainer, A Leitenstorfer and G H Döhler, *Europhys. Lett.* **70**, 534 (2005)

[7] G H Döhler, F Renner, O Klar, M Eckardt, A Schwanhäußer, S Malzer, D Driscoll, M Hanson, A C Gossard, G Loata, T Löffler and H Roskos, *Semicond. Sci. Technol.* **20**, S178 (2005)